

High-spin states in ^{152}Gd

S. Wang, H. Hua,* J. Meng, Z. H. Li, S. Q. Zhang, F. R. Xu, H. L. Liu, Y. L. Ye, D. X. Jiang, T. Zheng, Q. J. Wang, Z. Q. Chen, C. E. Wu, G. L. Zhang, D. Y. Pang, J. Wang, J. L. Lou, B. Guo, and G. Jin
School of Physics and MOE Key Laboratory of Heavy Ion Physics, Peking University, Beijing 100871, China

S. G. Zhou

*Institute of Theoretical Physics, Chinese Academy of Sciences, Beijing 100080, China
 and Center of Theoretical Nuclear Physics, National Laboratory of Heavy Ion Accelerator, Lanzhou 730000, China*

L. H. Zhu, X. G. Wu, G. S. Li, S. X. Wen, C. Y. He, X. Z. Cui, and Y. Liu
China Institute of Atomic Energy, Beijing 102413, China

(Received 15 April 2005; published 30 August 2005)

High-spin states of ^{152}Gd have been studied via the $^{148}\text{Nd}(^9\text{Be},5n)^{152}\text{Gd}$ fusion-evaporation reaction at a beam energy of 54 MeV. The ground-state band, octupole band, and β band have been extended up to spins 20^+ , 21^- , and 16^+ , respectively. A possible aligned two quasineutron band, which becomes the yrast band above the spin 16^+ , was observed for the first time. The kinematic behaviors of the ground-state bands and yrast bands in $^{152,154}\text{Gd}$ indicate that the shape of ^{152}Gd may change with increasing rotational frequency and the difference of quadrupole deformations between ^{152}Gd and ^{154}Gd obviously reduces around the first band crossing region. These observations are consistent with the theoretical calculations using cranked Woods-Saxon-Strutinsky methods. The first band crossing observed in ^{152}Gd can be ascribed to the alignment of a pair of $i_{13/2}$ neutrons. The identical ground-state bands in ^{152}Gd and ^{154}Dy were extended.

DOI: [10.1103/PhysRevC.72.024317](https://doi.org/10.1103/PhysRevC.72.024317)

PACS number(s): 21.10.Re, 23.20.Lv, 27.70.+q

I. INTRODUCTION

For the light rare-earth nuclei around mass $= 150$, the valence nucleons begin to fill $i_{13/2}$ neutron and $h_{11/2}$ proton orbitals. Nuclear deformations have a rapid transition from a spherical shape in closed shell to a prolate deformation in the neutron-rich region. Thus, the study of the properties of these transitional nuclei serves as an important test for various theoretical models. Theoretical studies of the ground-state properties of nuclei over a wide range of isospin have been made in an attempt to obtain a general description of shape transitions and to understand systematically the microscopic origin of these interesting phenomena [1–4].

High-spin studies of these transitional nuclei, which can give us a straightforward interpretation in terms of the interplay between the single-particle and collective degrees of freedom, have attracted a lot of experimental and theoretical attention. Many interesting phenomena have been observed in these nuclei with increasing spin, such as the prolate to oblate shape changes and band terminations. Since no suitable stable target/heavy-ion beam combinations are available to populate ^{152}Gd nucleus via the dominant xn decay channels in fusion-evaporation reactions, the excited states in ^{152}Gd have not been studied as high as those in its neighboring $N = 88$ isotones ^{150}Sm and ^{154}Dy . Here, we report a study of high-spin states in ^{152}Gd , which are populated by the $^{148}\text{Nd}(^9\text{Be},5n)^{152}\text{Gd}$ fusion-evaporation reaction.

II. EXPERIMENT

The present experiment was performed at the HI-13 tandem facility of the China Institute of Atomic Energy (CIAE) by bombarding a ^{148}Nd target with a ^9Be beam. Excited states in ^{152}Gd were populated through the $^{148}\text{Nd}(^9\text{Be},5n)^{152}\text{Gd}$ fusion-evaporation reaction. The target was a ^{148}Nd metallic foil enriched to 93.2% with a thickness of 1.1 mg/cm^2 . It is on a 1.1 mg/cm^2 carbon backing. The deexcitation γ rays were detected by 14 high-purity germanium (HPGe) detectors with BGO anti-Compton suppressors. These Compton-suppressed detectors were placed at angles of $44.6^\circ(4)$, $54.7^\circ(1)$, $90.0^\circ(4)$, $125.3^\circ(1)$, and $135.4^\circ(4)$ to the beam direction, where the numbers in parentheses indicate the number of detectors at that particular angle. The energy resolutions of these HPGe detectors were 2.0–2.5 keV at 1.33 MeV. All these detectors were calibrated using standard ^{152}Eu and ^{133}Ba γ -ray sources.

To determine the optimum beam energy for producing ^{152}Gd , γ -ray excitation functions were measured using beam energies of 42, 45, 48, 52, and 55 MeV. The experimental excitation functions for some intense γ rays observed in this experiment and the PACE4 program calculations for the fusion-evaporation cross sections are presented in Fig. 1. It shows that the excitation functions for the known 344.3, 411.1, 472.0, 519.4, and 553.6 keV transitions in ^{152}Gd have a similar trend as a function of beam energy and a largest yield around 55 MeV, which are in good agreement with the predictions of the PACE4 program. The γ - γ coincidence measurements were performed at a beam energy of 54 MeV. A total of 1.1×10^8 coincident events were collected, from which a symmetric γ - γ matrix was built. The level scheme analysis was performed using the RADWARE program [5]. The γ -ray spectra

*Corresponding author: Hhua@hep.pku.edu.cn

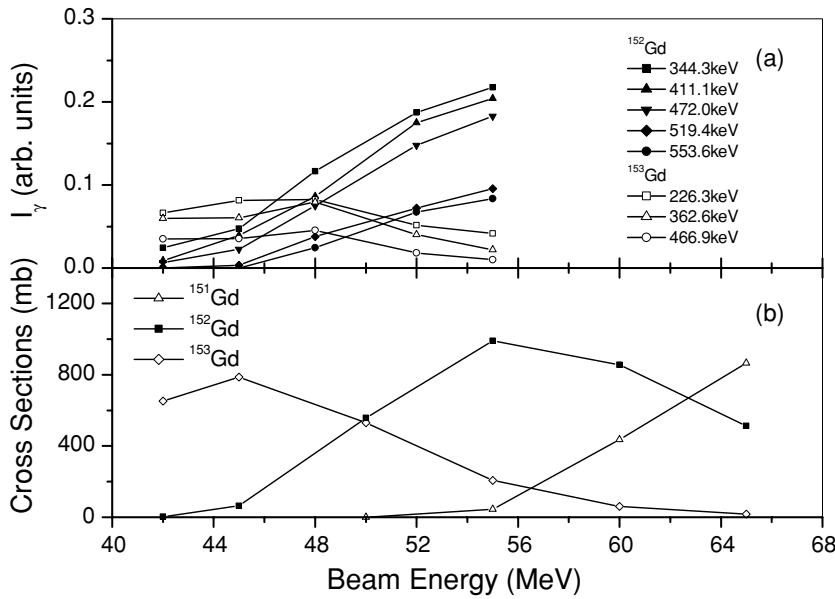


FIG. 1. (a) Excitation functions for the γ -ray transitions observed in the $^{148}\text{Nd}(^9\text{Be}, xn)$ reactions and (b) calculated cross sections using the PACE4 program for the $^{148}\text{Nd}(^9\text{Be}, xn)$ reactions.

gated on the known γ -ray transitions in ^{152}Gd are shown in Fig. 2. To obtain the directional correlations of γ -ray de-exciting oriented states (DCO) intensity ratios to determine the multiplicities of γ -ray transitions, the detectors at 90.0° with respect to the beam direction were sorted against the detectors at 135.4° to produce a two-dimensional angular correlation matrix. In general, stretched quadrupole transitions were adopted if DCO ratios were larger than 1.0, and stretched dipole transitions were assumed if DCO ratios were less than 0.8.

III. RESULTS AND DISCUSSION

In the previous study, the ground-state band in ^{152}Gd was established up to spin 16^+ at 4.143 MeV via $^{152}\text{Sm}(\alpha, 4n)^{152}\text{Gd}$ and $^{150}\text{Sm}(\alpha, 2n)^{152}\text{Gd}$ reactions, as well as the octupole band and β band up to spin 17^- at 4.609 MeV and spin 10^+ at

2.691 MeV, respectively [6–8]. The partial level scheme of ^{152}Gd , deduced from the current work, agrees with those previous results and is shown in Fig. 3. It was constructed from γ - γ coincidence relationships, intensity balances, and DCO analyses. The results are summarized in Table I. The ground-state band of ^{152}Gd was extended to spin 20^+ at 5.551 MeV. The octupole band was extended to spin 21^- at 6.082 MeV, and the β band was extended to spin 16^+ at 4.196 MeV. A possible odd-spin positive-parity aligned band in ^{152}Gd has been established by Zolnowski *et al.* [8]. Two more new levels were added to this band in the present work. By requiring a coincidence with the known γ -ray transitions below spin 16^+ of the ground-state band in ^{152}Gd , two new coincident γ -ray transitions of 604.8 and 639.7 keV were observed in the γ -ray spectra, one of which is shown in Fig. 2(a). The DCO ratio analyses suggest that both of them have quadrupole transition characters. Here, we tentatively assigned

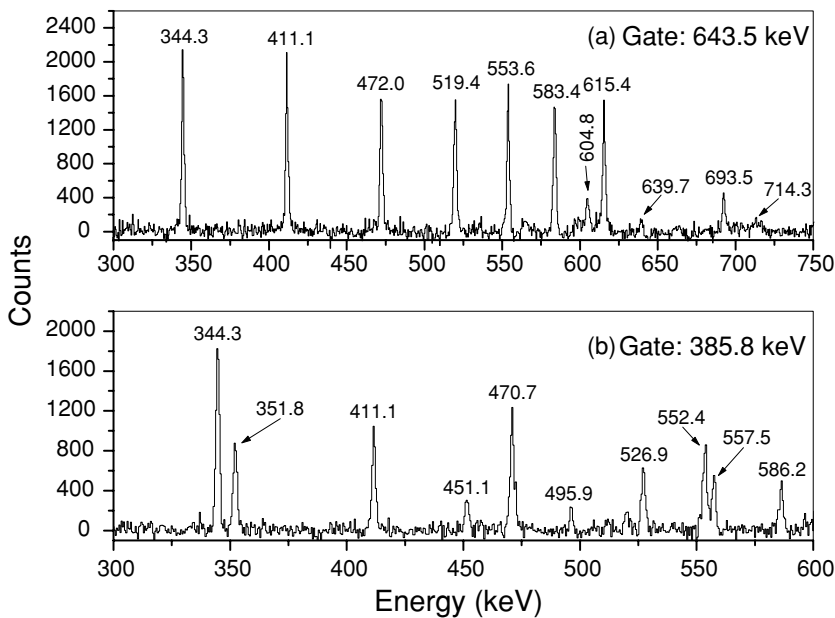


FIG. 2. Coincident γ -ray spectra with gating on (a) 643.5 keV transition and (b) 385.8 keV transition.

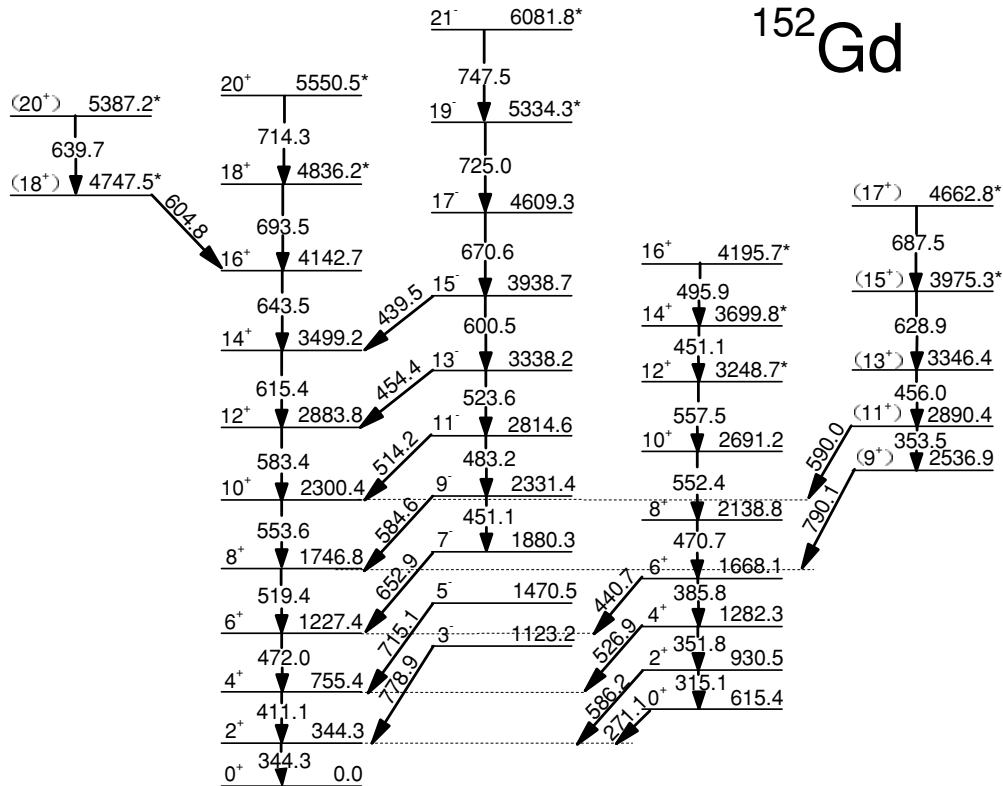


FIG. 3. Partial level scheme of ^{152}Gd . Energies are in keV. New levels observed in the current work are labeled with stars.

the 4.748 and 5.387 MeV level states, which relate to these two new sequential γ -ray transitions, to be spin 18^+ and spin 20^+ , respectively. In the neighboring isotope ^{154}Gd , an aligned two quasineutron band has been confirmed [9] and was found to become the yrast band above spin 16^+ . The similar γ -ray transition sequence and spin at which band crossing occurs compared to ^{154}Gd make us believe that the 4.748 and 5.387 MeV level states may also belong to an aligned two quasineutron band. More discussion of this new band will be given later.

The high-spin states, extended by the present work, allow a study of the band crossing phenomena and structure evolution along with spin in ^{152}Gd . The kinematic moments of inertia for the ground-state bands and yrast bands in $^{152,154}\text{Gd}$ as a function of rotational frequency are shown in Fig. 4(a). To identify the nature and origin of the observed band crossings, the kinematic moments of inertia for the bands, which are based on the $\nu i_{13/2}$ neutron excitation in ^{153}Gd [10] and the $\pi h_{11/2}$ proton excitation in ^{153}Tb [11], respectively, are plotted in Fig. 4(b). In the lower part of Fig. 4(a), the moments of inertia for the ground-state bands in ^{152}Gd and ^{154}Gd show a different dependence on the rotational frequency. The moment of inertia J_1 for ^{152}Gd increases rapidly compared with that of ^{154}Gd . After the band crossings around a frequency of ≈ 0.31 MeV, the moments of inertia for yrast bands in $^{152,154}\text{Gd}$ are close to each other and approach the rigid-rotor limit, where the continuations of the ground-state bands in $^{152,154}\text{Gd}$ also show similar behaviors. Since the $^{152,154}\text{Gd}$ have different quadrupole deformations ($\beta_2 = 0.205, 0.234$,

respectively [1]), the different moments of inertia in the lower part between these two isotopes are possibly caused by the difference in their quadrupole deformations. Also, the ^{152}Gd nucleus lies in the spherical to prolate shape transitional region. Its intrinsic structure is easily changed by the rapid rotation, especially the alignment of a high- j intruder nucleon pair, which is already observed in the neighboring $N = 88$ isotone ^{154}Dy [12]. Here, to get a further understanding of the effect of collective rotation on the microscopic structure in ^{152}Gd , cranked Woods-Saxon-Strutinsky calculations for $^{152,154}\text{Gd}$ have been performed by means of total-Routhian-surface (TRS) methods in a three-dimensional deformation space (β_2, γ, β_4) [13,14]. At a given frequency, the deformation of a state is determined by minimizing the calculated TRS. Figure 5 shows the results of TRS calculations for the yrast sequence of ^{152}Gd . It can be seen that the quadrupole deformation of ^{152}Gd changes from $\beta_2 = 0.205$ to $\beta_2 = 0.222$ with the rotational frequency increasing from 0.20 to 0.40 MeV, while the quadrupole deformation of ^{154}Gd was found to be stable as a function of rotational frequency. The difference of quadrupole deformations between ^{152}Gd and ^{154}Gd obviously reduces around the first band crossing region. So the similar kinematic behaviors observed in the upper part of Fig. 4(a) for $^{152,154}\text{Gd}$ may be a manifestation of similar quadrupole deformations for them at high rotational frequency.

In Ref. [9], the first band crossing occurring in ^{154}Gd can be ascribed to the alignment of a pair of $i_{13/2}$ neutrons. The similar crossing frequency observed in ^{152}Gd and ^{154}Gd , coupled with an alignment at similar rotational frequency observed in the

TABLE I. γ -ray energies, excitation energies, relative γ -ray intensities, and DCO ratios in ^{152}Gd .

E_γ (keV)	E_i (keV)	E_f (keV)	Int. (%)	DCO ratio	Assignment
271.1	615.4	344.3			$0^+ \rightarrow 2^+$
315.1	930.5	615.4			$2^+ \rightarrow 0^+$
344.3	344.3	0	100		$2^+ \rightarrow 0^+$
351.8	1282.3	930.5	3.7(0.2)	1.69(0.33)	$4^+ \rightarrow 2^+$
353.5	2890.4	2536.9			$(11^+) \rightarrow (9^+)$
385.8	1668.1	1282.3	5.7(0.2)	1.72(0.27)	$6^+ \rightarrow 4^+$
411.1	755.4	344.3	83.5(3.1)	1.50(0.09)	$4^+ \rightarrow 2^+$
439.5	3938.7	3499.2			$15^- \rightarrow 14^+$
440.7	1668.1	1227.4			$6^+ \rightarrow 6^+$
451.1	2331.4	1880.3			$9^- \rightarrow 7^-$
451.1	3699.8	3248.7	1.3(0.1)		$14^+ \rightarrow 12^+$
454.4	3338.2	2883.8			$13^- \rightarrow 12^+$
456.0	3346.4	2890.4	6.4(0.5)	1.92(0.18)	$(13^+) \rightarrow (11^+)$
470.7	2138.8	1668.1	4.9(0.4)	1.97(0.50)	$8^+ \rightarrow 6^+$
472.0	1227.4	755.4	65.0(5.0)	1.50(0.08)	$6^+ \rightarrow 4^+$
483.2	2814.6	2331.4	3.8(0.3)	1.33(0.19)	$11^- \rightarrow 9^-$
495.9	4195.7	3699.8	1.5(0.1)	1.34(0.45)	$16^+ \rightarrow 14^+$
514.2	2814.6	2300.4	9.1(0.6)	1.07(0.09)	$11^- \rightarrow 10^+$
519.4	1746.8	1227.4	48.7(3.3)	1.31(0.15)	$8^+ \rightarrow 6^+$
523.6	3338.2	2814.6	10.1(0.7)	1.48(0.24)	$13^- \rightarrow 11^-$
526.9	1282.3	755.4	2.2(0.2)	0.63(0.29)	$4^+ \rightarrow 4^+$
552.4	2691.2	2138.8	3.3(0.2)	>1	$10^+ \rightarrow 8^+$
553.6	2300.4	1746.8	37.2(2.2)	1.57(0.19)	$10^+ \rightarrow 8^+$
557.5	3248.7	2691.2	1.7(0.1)	>1	$12^+ \rightarrow 10^+$
583.4	2883.8	2300.4	16.8(0.8)	1.65(0.67)	$12^+ \rightarrow 10^+$
584.6	2331.4	1746.8	6.8(0.3)	0.74(0.35)	$9^- \rightarrow 8^+$
586.2	930.5	344.3	1.7(0.1)		$2^+ \rightarrow 2^+$
590.0	2890.4	2300.4	2.2(0.1)	1.51(0.24)	$(11^+) \rightarrow 10^+$
600.5	3938.7	3338.2	8.7(1.3)	1.54(0.18)	$15^- \rightarrow 13^-$
604.8	4747.5	4142.7	1.3(0.1)	1.70(0.43)	$(18^+) \rightarrow 16^+$
615.4	3499.2	2883.8	6.9(1.0)	1.55(0.25)	$14^+ \rightarrow 12^+$
628.9	3975.3	3346.4	3.2(0.1)	>1	$(15^+) \rightarrow (13^+)$
639.7	5387.2	4747.5	1.0(0.1)	1.49(0.41)	$(20^+) \rightarrow (18^+)$
643.5	4142.7	3499.2	3.1(0.1)	1.62(0.90)	$16^+ \rightarrow 14^+$
652.9	1880.3	1227.4	3.8(0.1)	0.94(0.23)	$7^- \rightarrow 6^+$
670.6	4609.3	3938.7	7.9(0.2)	1.60(0.32)	$17^- \rightarrow 15^-$
687.5	4662.8	3975.3	1.3(0.1)	>1	$(17^+) \rightarrow (15^+)$
693.5	4836.2	4142.7	1.3(0.1)	1.58(0.44)	$18^+ \rightarrow 16^+$
714.3	5550.5	4836.2	0.7(0.1)	>1	$20^+ \rightarrow 18^+$
715.1	1470.5	755.4			$5^- \rightarrow 4^+$
725.0	5334.3	4609.3	1.8(0.1)	1.23(0.20)	$19^- \rightarrow 17^-$
747.5	6081.8	5334.3	0.5(0.1)	1.32(0.56)	$21^- \rightarrow 19^-$
778.9	1123.2	344.3			$3^- \rightarrow 2^+$
790.1	2536.9	1746.8	2.1(0.1)		$(9^+) \rightarrow 8^+$

band on the $\pi h_{11/2}$ proton level in ^{153}Tb and the blocking effect observed in the band on the $\nu i_{13/2}$ neutron level in ^{153}Gd , indicates that the $i_{13/2}$ neutron-pair alignment is also responsible for the band crossing in ^{152}Gd . Band crossing phenomena in ^{154}Gd have been studied using the cranked shell model [9]. Our TRS calculations for the yrast sequence of ^{152}Gd predict a rapid increase in aligned angular momentum due to a neutron-pair alignment around the rotational frequency 0.30 MeV, which is in good agreement with the experimental value for ^{152}Gd . It provides a complementary confirmation for the cause of

the first band crossing in ^{152}Gd . The TRS calculations also predict that the $h_{11/2}$ proton-pair alignment in ^{152}Gd occurs in the vicinity of rotational frequency 0.40–0.45 MeV. It is already experimentally found in the neighboring Dy, Er, and Yb nuclei [9].

One interesting observation in this work is that the nearby identical ground-state bands in ^{152}Gd and ^{154}Dy [8] were kept up to the band cross region with two more new level states added to the ground-state band in ^{152}Gd . The energy differences between γ -ray transitions for the ground-state

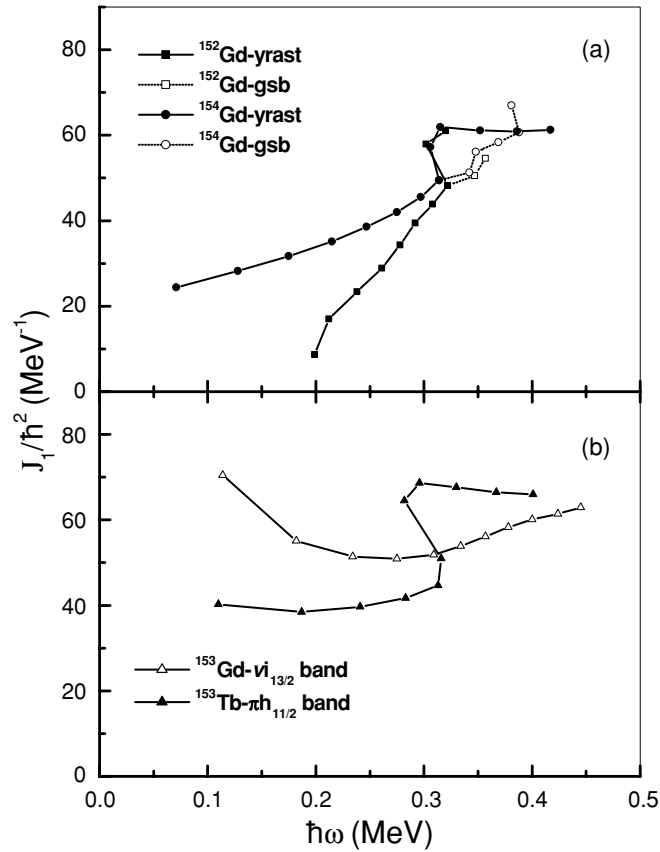


FIG. 4. Kinematic moments of inertia as a function of the rotational frequency for (a) yrast bands and ground-state bands in $^{152,154}\text{Gd}$ and (b) $vi_{13/2}$ band in ^{153}Gd and $\pi h_{11/2}$ band in ^{153}Tb .

bands in ^{152}Gd and ^{154}Dy are plotted in Fig. 6. Except the data at spin 16^+ , the ground-state bands are identical within 10 keV in these two nuclei. The identical bands were also seen in the neighboring odd- A ^{153}Gd and ^{155}Dy nuclei [10], as well as in the even- A ^{152}Sm [15] and ^{154}Gd [9] nuclei,

which are shown in Fig. 6. Detailed studies of the extended identical bands in these two transitional nuclei, combined with the studies of identical bands in their neighboring nuclei with stable deformations, will provide insight into the origin of identical bands.

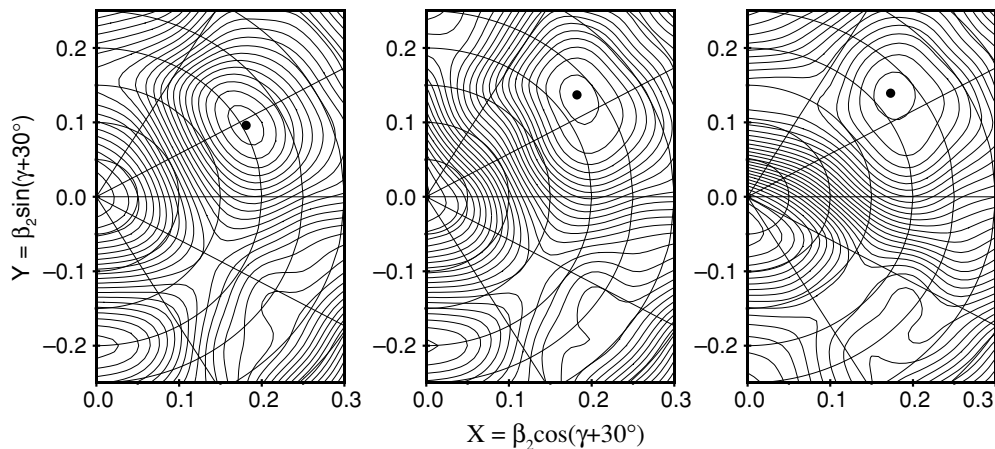


FIG. 5. TRS calculations for yrast sequence in ^{152}Gd . Energy contours are at 200 keV intervals. Deformation parameters for the individual minima are left: $\hbar\omega = 0.20$ MeV, $\beta_2 = 0.205$, $\gamma = -2.1^\circ$, and $\beta_4 = 0.042$; middle: $\hbar\omega = 0.30$ MeV, $\beta_2 = 0.227$, $\gamma = 7.0^\circ$, and $\beta_4 = 0.049$; right: $\hbar\omega = 0.40$ MeV, $\beta_2 = 0.222$, $\gamma = 8.7^\circ$, and $\beta_4 = 0.041$.

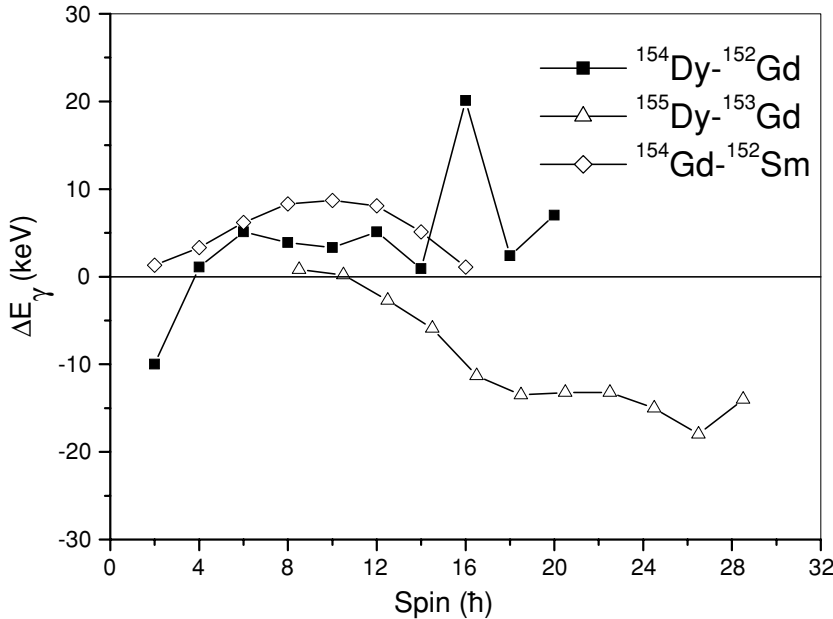


FIG. 6. Energy differences of corresponding γ -ray transitions in neighboring even- A and odd- A isotones.

IV. SUMMARY

With the ^9Be beam provided by the HI-13 tandem accelerator of the China Institute of Atomic Energy, high-spin states of ^{152}Gd have been studied via the $^{148}\text{Nd}(^9\text{Be},5n)^{152}\text{Gd}$ fusion-evaporation reaction. The ground-state band, octupole band, and β band have been extended up to spins 20^+ , 21^- , and 16^+ , respectively. A new possible aligned two quasineutron band, which becomes the yrast band above the spin 16^+ , was observed. The kinematic behaviors of the ground-state bands and yrast bands in $^{152,154}\text{Gd}$ indicate that the quadrupole deformation of transitional nucleus ^{152}Gd changes with increasing rotational frequency and the difference of quadrupole deformations between ^{152}Gd and ^{154}Gd obviously reduces around the band crossing region, which are consistent with the total Routhian surface calculations for $^{152,154}\text{Gd}$. The

first band crossing observed in ^{152}Gd can be ascribed to the alignment of a pair of $i_{13/2}$ neutrons. The identical ground-state bands in ^{152}Gd and ^{154}Dy were extended. To confirm the possible quadrupole deformation changes along with the rotational frequency in ^{152}Gd , more experimental work is needed.

ACKNOWLEDGMENTS

The authors wish to thank Prof. G. J. Xu for making the target and the staffs in the tandem accelerator laboratory at the China Institute of Atomic Energy (CIAE), Beijing. This work is support by the National Natural Science Foundation of China (10405001, 10475002, 10475003, 10221003) and the Major State Basic Research Development Program (G2000077400).

-
- [1] W. Nazarewicz, M. A. Riley, and J. D. Garrett, Nucl. Phys. **A512**, 61 (1990).
- [2] P. Moller, J. R. Nix, W. D. Myers, and W. J. Swiatecki, At. Data Nucl. Data Tables **59**, 185 (1995).
- [3] G. A. Lalazissis, M. M. Sharmab, and P. Ring, Nucl. Phys. **A597**, 61 (1996).
- [4] G. A. Lalazissis, S. Raman, and P. Ring, At. Data Nucl. Data Tables **71**, 1 (1999).
- [5] D. C. Radford, Nucl. Instrum. Methods Phys. Res. A **361**, 297 (1995).
- [6] D. R. Zolnowski, T. Kishimoto, Y. Gono, and T. T. Sugihara, Phys. Lett. **B55**, 453 (1975).
- [7] M. Guttormsen, J. Rekestad, and L. L. Riedinger, Phys. Scr. **22**, 210 (1980).
- [8] D. R. Zolnowski, M. B. Hughes, J. Hunt, and T. T. Sugihara, Phys. Rev. C **21**, 2556 (1980).
- [9] J. D. Morrison, J. Simpson, M. A. Riley, H. W. Granmer-Gordon, P. D. Forsyth, D. Howe, and J. F. Sharpey-Schafer, J. Phys. G **15**, 1871 (1989).
- [10] T. B. Brown, M. A. Riley, D. Campbell, D. J. Hartley, F. G. Kondev, J. Pfohl, R. V. F. Janssens, S. M. Fischer, D. Nisius, P. Fallon, W. C. Ma, J. Simpson, and J. F. Sharpey-Schafer, Phys. Rev. C **66**, 064320 (2002).
- [11] D. J. Hartley, T. B. Brown, F. G. Kondev, R. W. Laird, J. Pfohl, A. M. Richmond, M. A. Riley, J. Doring, and J. Simpson, Phys. Rev. C **58**, 1321 (1998).
- [12] W. C. Ma, M. A. Quader, H. Emling, T. L. Khoo, I. Ahmad, P. J. Daly, B. K. Dichter, M. Drigert, U. Garg, Z. M. Grabowski, R. Holzmann, R. V. F. Janssens, M. Piiparinen, W. H. Trzaska, and T.-F. Wang, Phys. Rev. Lett. **61**, 46 (1988).
- [13] W. Satula, R. Wyss, and P. Magierski, Nucl. Phys. **A578**, 45 (1994).
- [14] F. R. Xu, W. Satula, and R. Wyss, Nucl. Phys. **A669**, 418 (2000).
- [15] J. Konijn, J. B. R. Berkhout, W. H. A. Hesselink, J. J. van Ruijven, P. van Nes, H. Verheul, F. W. N. de Boer, C. A. Fields, E. Sugarbaker, P. M. Walker, and R. Bijker, Nucl. Phys. **A373**, 397 (1982).